![GeoVirtual 2020 September 14-16 Resilience and Innovation]

Calibration of the Hardening Soil Small Strain Constitutive Model Parameters for Toronto Glacial Till

Evan Sau Yue Ma[1], Mei T. Cheong[1], Sergei Terzaghi[2].
[1]Arup Canada Inc., Toronto, Ontario, Canada
[2]Arup Australasia, Sydney, Australia

ABSTRACT
The Finch West Light Rail Transit infrastructure project proposed in Toronto requires construction of deep retaining walls with excavations into approximately 18m of glacial till of the Halton geologic unit, consisting of silty clay and sandy silt. An advanced finite element constitutive soil model, the PLAXIS Hardening Soil with Small Strain (HSs) model, was used to perform soil-structure interaction analysis. The model was calibrated with laboratory and field test data, which comprised isotropically consolidated, drained and undrained triaxial compression, oedometer, and geophysics. This study summarizes the range of HSs model input parameters that are applicable for the project geology. The HSs model predictions were validated using two methods: the model predicted undrained shear strength was found to be comparable with the TEXAM Pressuremeter field measurements, and the model predicted shoring wall deflections were found to be comparable to inclinometer data from a historical excavation in similar geology.

RÉSUMÉ
Le projet Finch West Light Rail Transit qui a proposé à Toronto nécessite la construction des murs de soutènement profonds et des excavations d'environ 18m de profondeur dans le till composé d'argile limoneuse et du limon sableux. Un modèle avancé de sol constitutif d'éléments finis avec le modèle <<PLAXIS Hardening Soil with Small Strain (HSs)>> a été utilisé pour effectuer une analyse d'interaction sol-structure. Le modèle a été étalonné au moyen des essais en laboratoire et d'essai in situ, composés des oedomètres, des géophysiques et des pressiomètres TEXAM. Cette étude résume les paramètres d'entrée pour le modèle HSs, qui sont applicables à la géologie du projet. Les prévisions du modèle HSs ont été validées à l'aide de deux méthodes: la résistance au cisaillement estimée par le modèle était comparable aux mesures de pressiomètre, et les mouvements du etayage estimés par le modèle étaient comparable aux données d'inclinométre et aux données d'une excavation ancienne qui est similaire de par sa géologie à Finch.

1   INTRODUCTION

The Metrolinx owned Finch West Light Rail Transit (FWLRT) Project comprises the design, construction and maintenance of a 11.5km Light Rail Transit (LRT) corridor in Toronto. The LRT corridor will run along the existing Finch Avenue West in an east-west direction. Two underground stations, Finch West Station (FWS) and Humber College Stop (HCS), and a Maintenance Storage Facility (MSF) are proposed for the project (See Figure 1).

The proposed station structure is located in close proximity to the existing Toronto Transit Commission (TTC) Finch West Station completed in 2017 as part of the Toronto-York-Spadina Subway Extension (TYSSE). The proposed layout of the FWS comprises a U-Portal west of Keele Street, which takes the tracks from Finch Avenue West into the station, consisting of a shallow cut and cover box beneath the Finch Avenue West and Keele Street intersection, and a deep station box at the eastern boundary. Two levels of excavation, shallow and deep, typically 10m and 16m deep (maximum 18m), are proposed. The support of excavation design consists of up to four levels of prestressed anchors and/or struts, utilizing both bottom up and top down construction methods. A plan of the proposed and existing TYSSE station is shown in Figure 2.
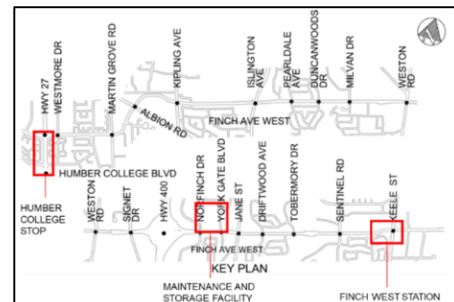

Figure 1. Key plan of Finch West LRT alignment

2   SCOPE AND BACKGROUND

2.1   SCOPE

An advanced finite element constitutive soil model, the PLAXIS Hardening Soil with Small Strain (HSs) model was used to perform non-linear ground movement analysis. This study presents the range of HSs model parameters that are applicable for the project in the local Toronto geology, and how these parameters can be derived from laboratory and field data. The paper shows the calibration of key parameters used in the HSs model. The model was validated by comparing the predictions with TEXAM Pressuremeter field measurements and with shoring movements measured from another local project.
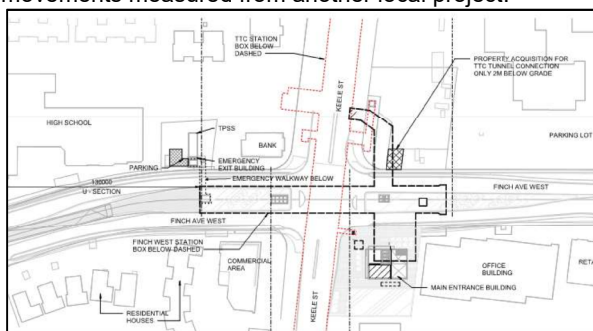

Figure 2. Plan showing outline of proposed and existing TYSSE Finch West station

2.2   Subsurface Stratigraphy

The Quaternary deposits of Toronto consist predominantly of glacial till-derived material. The proposed Finch West Station is located within the young till deposit in Toronto known as the Halton Unit. The younger tills in the Toronto area were deposited in the late Wisconsinan time when the glaciers returned once again after deposition of older tills during the Illinoisan Stage, early and mid Wisconsinan. A historical river channel, with sand and gravel deposits, flows southwards toward Lake Ontario meandering to the west as it approaches the intersection at Finch Avenue West and Keele Street.

2.3   Finch West Station Stratigraphy

The FWS site is typically underlain by up to 3m of Fill overlying 9 to 14m of cohesive glacial till, and 2 to 3m of cohesionless glacial till, which are underlain by up to 8m thick lenses of glacio-fluvial sand deposits. The cohesive glacial till is generally formed of clayey silt and silty clay till, and trace gravel, and is brown to grey in color, firm to hard, and typically very stiff to depths of 15m and typically hard below 15m. The cohesive till is of low plasticity, and is not sensitive to shear in remoulding. Groundwater level is at approximately 1.5m below existing ground.

2.4   Site Investigation and Testing

Recent site investigation for the FWLRT project was completed between 2016 and 2019. Auger drilling and sampling was completed along the route, with laboratory testing completed primary at the MSF and the FWS. Historical ground investigation for the TYSSE project was completed in 2010. This paper uses data from both the current proposed FWLRT project, as well as the data that was obtained from previous historical investigation for the existing TYSSE station.

The recent site investigation included Index testing, including natural moisture content (w_n), plasticity index (PI), and Standard Penetration Test (SPT). Laboratory testing consisted of Consolidated Isotropically, drained (CIDC), and undrained (CIUC) triaxial, and 1D incrementally loaded oedometer tests. Field testing included geophysical acoustic velocity measurements, and TEXAM Pressuremeter.

Figure 3 shows the index testing at FWS, and the simplified stratigraphic model. Figure 4 shows the compressibility parameters, and stress history parameters from oedometer tests. A summary is presented in Table 1.
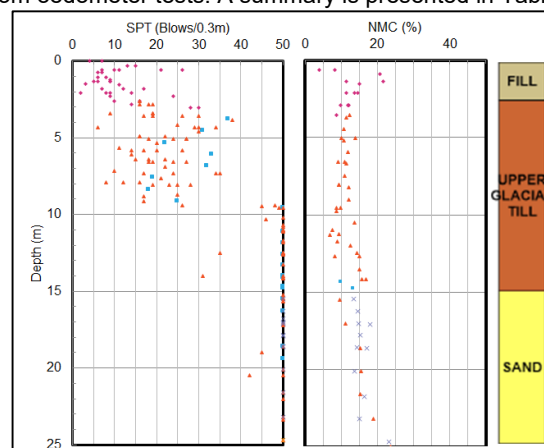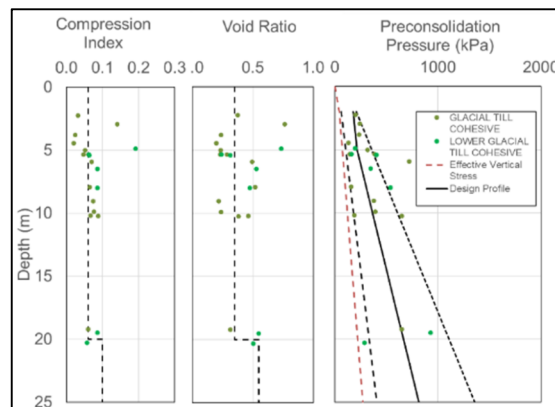

Figure 3. Index Testing at Finch West Station

Figure 4. Compressibility and Stress History Parameters

Table 1. Summary of Index and Stress History Parameters

Stratum	NMC (%)	SPT (blows /ft)	Plasticity (%)	OCR
Fill	13%±5	12±7	-	-
Cohesive Upper Glacial Till	12%±3	33±15	7±3	2-5
Cohesionless Upper Glacial Till	12%±2	42±12	-	-
Sand	16%±3	50+	-	-

3 CALIBRATION OF HARDENING-SOIL-SMALL STRAIN MODEL

The HSs model is a rate-independent, hyperbolic, isotropic hardening, effective stress constitutive model. Some basic characteristics of the model include stress-dependency of stiffness, plastic straining due to primary deviatoric loading, plastic straining due to primary compression, elastic unloading/reloading, and failure according to the Mohr-Coulomb criteria. For non-sensitive, strain hardening clay tills in Toronto, this model is applicable for strutted excavations where the analysis is highly influenced by the non-linear stiffness of soil. The required input parameters for the model are shown in Table 2. The following sections describe how each of the PLAXIS input parameters were derived from the available laboratory test results.

Table 2. Hardening Soil with Small Strain Model Inputs

Parameter	Description	Parameter Evaluation
$E_{50,ref}$	Reference secant stiffness in primary loading (deviatoric shearing at the yield envelope) from drained triaxial test	y-intercept in $\log(\sigma_3/p_{ref}) - \log(E_{50})$ space
$E_{oed,ref}$	Reference tangent stiffness from primary (virgin compression) oedometer loading	y-intercept in $\log(\sigma_3/p_{ref}) - \log(E_{oed})$ space
$E_{ur,ref}$	Reference unloading/reloading stiffness	y-intercept in $\log(\sigma_3/p_{ref}) - \log(E_{ur})$ space
m	Stress dependency according to the power law	Slope of trendline $\log(\sigma_3/p_{ref}) - \log(E_{50})$ space
$G_{max,ref}$	Reference maximum strain shear modulus from	Shear Wave
$\gamma_{0.7}$	Shear strain at 0.7 G_{max}	Reference
ϕ'	Effective friction angle	Triaxial
c'	Effective Cohesion	Triaxial
ψ	Dilatancy angle	Triaxial
R_f	Failure ratio	Triaxial
v_{ur}	Unloading/reloading Poisson's ratio	0.2 (default)
$K_{0,nc}$	Coefficient of earth pressure at rest at normally consolidation	1-sinϕ'

3.1 Reference Secant Stiffness ($E_{50,ref}$) from Triaxial

The drained secant Young's Modulus, E'_{50}, which is defined as the secant modulus at 50% of the maximum deviatoric stress in a triaxial test under primary loading, controls the deviatoric plastic straining in the HSs model. This parameter was obtained from drained and undrained, isotropically consolidated triaxial test (CIDC; CIUC). In the case of the CIUC tests, the undrained modulus was corrected for drained stiffness by the following relationship:

$$E' = \frac{2(1 + v')E_u}{3} \qquad [1]$$

The determination of E_{50}, or E_{ur} in the HSs model requires the input of an arbitrary reference pressure, p_{ref} for stress dependency of stiffness according to the following relationship:

$$E_{50\ or\ ur} = E^{ref}_{E50\ or\ ur}\left(\frac{c\ cos\varphi - \sigma'_3 sin\varphi}{c\ cos\varphi + p'_{ref} sin\varphi}\right)^m \qquad [2]$$

For simplicity, this paper will define p_{ref} = 100 kPa (i.e. atmospheric pressure). E_{oed} and G_{max} can be related to the p_{ref} and friction angle by similar relationships.

The secant stiffness, E_{50}, and stress dependency parameter, m, was obtained by plotting the secant stiffness against the consolidation pressure, normalized by p_{ref} on a double log plot. The reference secant stiffness, $E_{50,ref}$ is the y-intercept of this construction, and the slope is the power-law, m, parameter. This is shown in Figure 5.
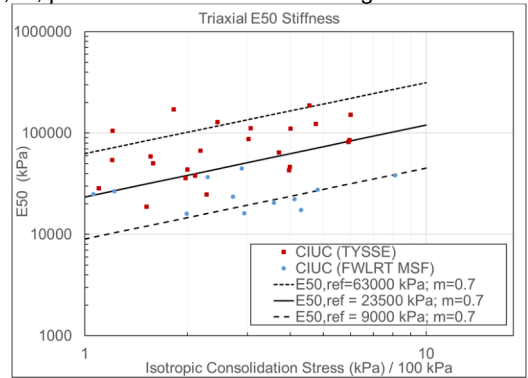

Figure 5. Triaxial Secant Modulus

3.2 Tangent Stiffness from Oedometer

The plastic straining due to primary virgin compression is a function of the tangent oedometer modulus, E_{oed}. The E_{oed} was obtained from a total of 31 oedometer tests at primary compression. The reference oedometer modulus, $E_{oed,ref}$ was obtained by plotting the data using double log scale as discussed previously, and is shown in Figure 6.
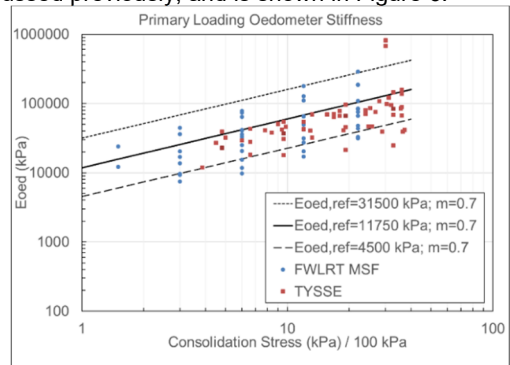

Figure 6. Primary Loading Oedometer Modulus

3.3 Unload/Reload Stiffness

The unload/reload stiffness parameter is defined as the stiffness obtained in a triaxial test in the unload/reload cycle. Typical E_{ur}/E_{50} value of 3 is published in the literature (Schanz, Vermeer, and Bonnier ,1999). It should be noted that higher E_{ur}/E_{50} (3 to 6) have been reported for softer clays, and loose sands, whereas lower E_{ur}/E_{50} (2 to 4) were reported for stiffer materials and denser cohesionless soil (Obrzud and Truty, 2018).

As the unload/reload cycles were not conducted as part of the triaxial tests for this project, the unload-reload modulus was obtained from the oedometer tests. The unload reload modulus from the oedometer is shown in Figure 7. The ratio of elastic unload/reload modulus to the loading modulus in compression was assumed to be equal to the elastic unload/reload modulus to the loading modulus in shear. The ratio was approximately 3, which was consistent with the literature.
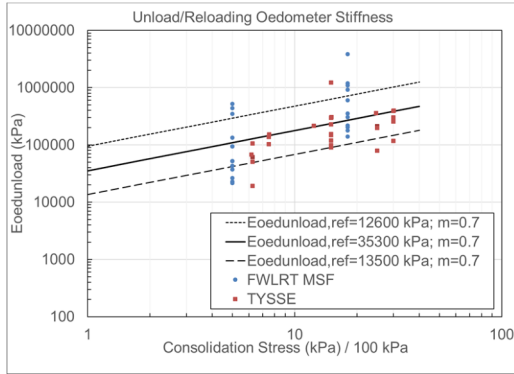

Figure 7. Elastic Unload/Reload Oedometer Modulus

3.4 Dynamic Small Strain Stiffness Parameters

Soil stiffness decreases and damping increases with shear strain. The damping and stiffness degradation characteristics of the HSs model is characterized by the Santos and Correia (2001) hyperbolic relationship:

$$\frac{G}{G_{max}} = \frac{1}{1 + 0.385\frac{\gamma}{\gamma_{0.7}}} \qquad [3]$$

The Gmax is the shear modulus at small strains and was estimated from geophysical field testing with the shear wave velocity, Vs, and the soil density, ρ, using the following equation:

$$G_{max} = \rho\, V_s^{\,2} \qquad [4]$$

Shear wave velocity, Vs, was estimated to be between 300m/s to 500m/s in the Glacial Till at Finch West Station. These values are slightly greater than the range of values reported by Cao (2015). The G_{max} based on the Vs values were plotted in a double-log plot and the effective stress normalized by p_{ref}, as shown in Figure 12 in order to obtain $G_{max,ref}$ @ p_{ref} = 100 kPa.
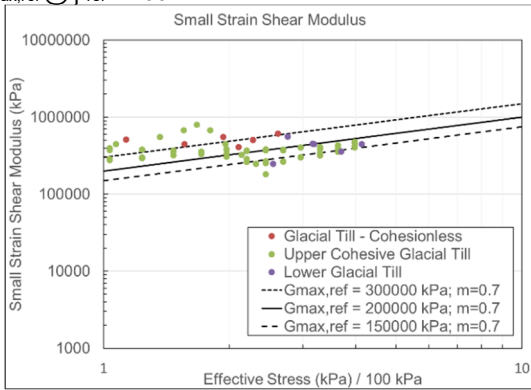

Figure 8. Small strain stiffness obtained from geophysics.

A site-specific continuous stiffness degradation curve was not available to accurately determine $\gamma_{0.7}$, shear strain at 0.7 Gmax. Naghavi et al. (2019) present results obtained from cyclic triaxial testing for shear strains larger than 0.1%, and resonant column testing for shear strains smaller than 0.1% on non-cohesive glacial till, and on sand/sandy silt on a TTC project. Naghavi et al. (2019) report $\gamma_{0.7}$ values ranging from 0.01% to 0.03%. The Authors selected this parameter to be 0.01%, on this basis for tills in Toronto and from the literature for fine grained soils (Vardanega and Bolton, 2011).

3.5 Strength parameters from Triaxial

The critical state friction angle, ϕ_{cs}, was obtained from an analysis of 15 sets of triaxial data. The triaxial data was plotted in p' = [(σ'$_1$+σ'$_3$)/2] vs. q = [(σ'$_1$- σ'$_3$)/2] space, as shown in Figure 9 with friction angles varying between 31° and 37° with c'=0. For the data set, the propensity of the triaxial results suggests a ϕ_{cs} of approximately 34 degrees and is consistent with local empirical correlations for the friction angle of glacial till (Cao, 2015). The peak friction angle obtained from triaxial testing was generally between 1° to 3° above, ϕ_{cs}.
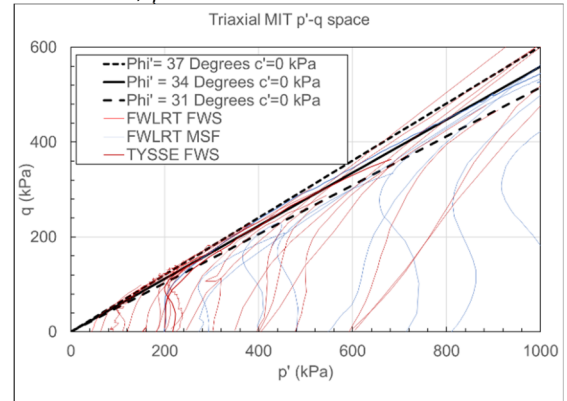

Figure 9. CIUC triaxial results in MIT p-q' space

The peak dilation angle, ψf, was obtained indirectly from the triaxial tests. From Bolton (1986), the peak dilation angle can be estimated as follows:

$$\phi_{peak} = 0.5\psi_f + \phi'_{cs} \qquad [5]$$

Therefore, a peak dilation angle can be estimated to range from 2° to 6°. For a triaxial sample consolidated isotropically to the same effective stress, the porewater pressure, and stress strain behavior is sensitive to the dilation angle. As an example, dilation angles of 2° and 5° were modelled using PLAXIS SoilTest, and shown to fit well with the set of triaxial data as shown in Figure 10.

The failure ratio, Rf is defined as the ratio of the deviatoric stress at failure and the asymptotic deviator stress for a hyperbolic curve. For primary loading (i.e. deviatoric shearing at the yield envelope, as defined in the PLAXIS manual) in drained triaxial, the hyperbolic relationship between deviatoric stress, and axial strain is expressed by Obrzud and Truty (2018) as follows:

$$\sigma_1 - \sigma_3 = \frac{\varepsilon_1}{\dfrac{1}{2E_{50}} + \dfrac{\varepsilon_1 R_f}{(\sigma_1 - \sigma_3)_f}} \qquad [6A]$$

Equation 6A can be rearranged into a linear form, y=mx+b:

$$\frac{\varepsilon_1}{\sigma_1 - \sigma_3} = \frac{1}{2E_{50}} + \varepsilon_1 \frac{R_f}{(\sigma_1 - \sigma_3)_f} \qquad [6B]$$
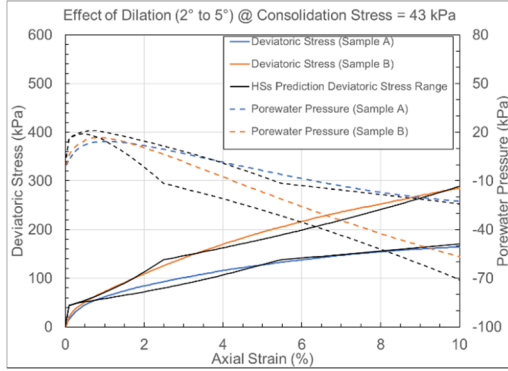

Figure 10. Effect of Dilation Angle

R_f can be obtained graphically by plotting $\varepsilon_1/(\sigma_1 - \sigma_3)$ as a function of ε_1. The slope of the line of best fit with a y-intercept at $1/2E_{50}$, is equal to $R_f/(\sigma_1 - \sigma_3)_f$. Therefore, R_f can be obtained by multiplying the slope by the deviatoric stress at failure. An example of this graphical construction is shown in Figure 11. The results of this analysis on the triaxial data set present the range of R_f values varying from 0.70 to 0.92, shown in Figure 12.
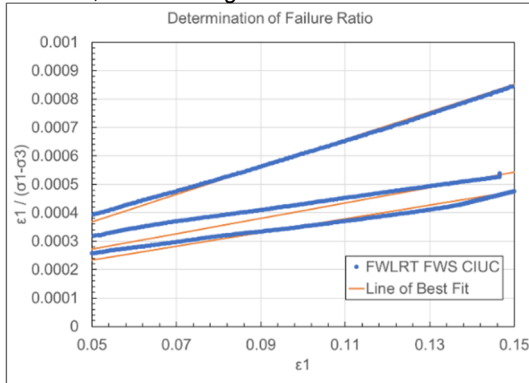

Figure 11. Graphical construction to determine failure ratio.

3.6 Hydraulic Conductivity

Additionally, permeability parameters are required for transient seepage or consolidation analyses. The hydraulic conductivity and consolidation properties of the cohesive glacial till were interpreted from the available slug and pumping well tests. The relationship between the coefficient of consolidation, c_v, and void ratio is linked with change in stress by the compression index, C_c as follows:

$$C_v = \frac{k_0(1 + e_0)\sigma'_{va}}{0.434 C_c \gamma_w} \qquad [7]$$

where σ'_{va} is the average vertical effective stress, and γ_w is the weight of water. Similarly, the hydraulic conductivity, k_v, also varies with void ratio, and is linked by the slope of the e vs. log k relationship:

$$C_k = \frac{e - e_0}{\log \frac{k_v}{k_0}} \qquad [8]$$

A review of the consolidation tests indicate that c_v is relatively constant throughout consolidation. Therefore, $C_k=C_c$ was assumed to ensure that c_v remains constant. On this basis, the Authors selected an average value, k_v=1.6x10-8 m/s for the glacial till, and a $C_k=C_c$=0.06.
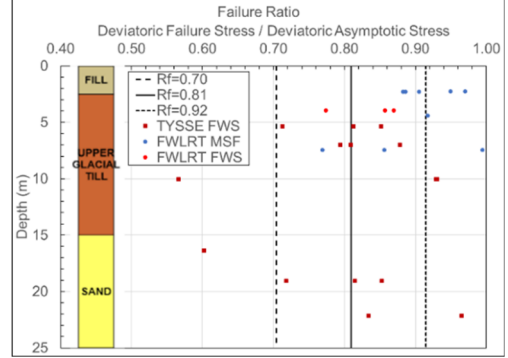

Figure 12. Failure ratio from triaxial analysis

4 RESULTS

4.1 Summary of Calibrated Design Parameters

Based on the above calibration, a summary of the suggested range of values for the HSs model input parameters are presented in Table 3. The following sections describe how the calibrated model predictions, using selected design input shown in Table 3, were validated with field, empirical, and historical data.

Table 3.Summary of calibrated parameters

Parameter	Suggested Range of Values	Selected Design Value
$E_{50,pref=100}$ (kPa)	9000 to 63000	23500
$E_{oed, pref=100}$ (kPa)	4500 to 31500	11750
$E_{ur, pref=100}$ (kPa)	27000 to 189000	70500
m	-	0.7
$G_{max,ref}$ (MPa)	150 to 300	200
$\gamma_{0.7}$ (%)	0.01 to 0.03	0.01
ϕ_{cs} (°)	31 to 36	34
c' (kPa)	0	0
ψ (°)	2 to 6	3
R_f	0.70 to 0.91	0.81
v_{ur}	-	0.2
$K_{0,nc}$	-	0.4408
$k_v=k_h$ (m/s)	-	1.6E-8
C_k	-	0.06
State Parameters		
OCR	2 to 5	3.0
K_0	-	0.66

4.2 Strength Validation

The calibrated HSs model was used to predict undrained shear strength measured using a TEXAM-type pressuremeter test conducted independently in the field. The predictions were generated in PLAXIS SoilTest using both the Direct Simple Shear (DSS) and triaxial (TX) test

methods and were presented to show the effect of undrained strength anisotropy. The undrained strength predictions from the HSs model were compared to the undrained shear strength measured using the TEXAM-type pressuremeter test, as shown in Figure 13.
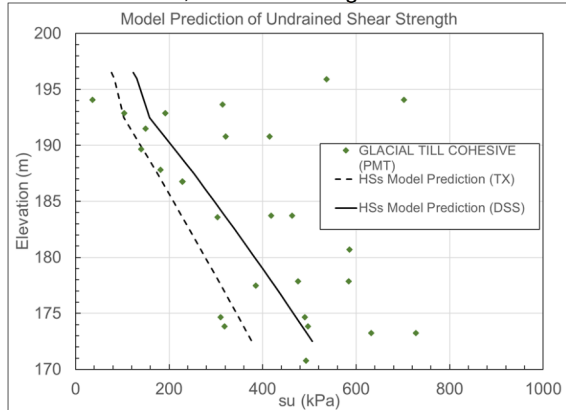

Figure 13. Model Prediction of Undrained Shear Strength and Field Testing values obtained by Pressuremeter

4.3   Stiffness Validation

As excavation of the proposed Finch West Station has not commenced at the time of writing, the calibrated HSs model was used to predict ground movement of the Sheppard-Yonge Station (SYS) Line 4 excavation completed in 2002. The model predictions were compared with historical SYS monitoring data published by Boone and Westland (2004).

The SYS is a deep braced excavation, located 6.5km south-east of the proposed Finch West Station, in similar Glacial Till geology to FWS. The ground stratigraphy at SYS was modelled as 2m of fill overlying Glacial Till using the calibrated HSs model with input parameters provided in Table 3. Groundwater was assumed at 6m below ground surface. The SYS excavation was modelled as 20m wide, with 3 levels of struts, and a deck beam. Struts and piles were spaced at 3m c/c apart, and the pile toe was modelled to be 3.5m below the base of excavation as per details provided by Boone and Westland (2004).

The structural details of the SYS support of excavation design was not reported by Boone and Westland. (2004), only the non-dimensional stiffness (S_r) was provided.

$$S_r = \frac{EI}{\gamma h^4} \qquad [9]$$

Where, EI is the flexural stiffness of the wall per length into the excavation, γ is the unit weight of soil, and h is the spacing between struts.

Several modelling assumptions were therefore made regarding the structural details. The S_r ratio used in the model was found to be between 17 and 56. These values were comparable to the S_r values reported for SYS. Therefore, the assumptions made in the model are considered to be comparable to the SYS shoring system.

It should be noted that while the original Sheppard Station design allowed for 50% pre-stressing load on the struts, Boone and Westland (2004) suggested poor

workmanship resulted in relaxation of the pre-stressing load immediately after installation during the first half of the project stages. Therefore, it was assumed that the prestress loading was only applied for the lowest strut in the back-analysis model, to reflect this sequencing.

Both transient seepage (assumed 300 construction days [CD]) and fully drained conditions were modelled to capture the uncertainty in the SYS construction period. It should be noted that the glacial till in Toronto may exhibit anisotropy (k_v/k_h=0.1). A sensitivity analysis was conducted using anisotropic hydraulic conductivity flow parameters. It was found that reducing the hydraulic conductivity in the vertical direction had little impact on the results for this study as the transient analysis was primarily governed by flow in the horizontal direction.

4.3.1   Validation against Ground Settlement

The predicted surface movements using the calibrated HSs model were compared against the SYS reported ground movements, and with local empirical correlations as shown in Figure 14. Comparison of the predicted movements with empirical ground movement criteria based on normalized settlement with excavation depth (Boone et al., 1998, Clough and O'Rourke, 1990), indicate that the numerical predictions correspond with the empirical normalized settlement curves for hard tills and very dense sand. It should be noted that the effects of groundwater drawdown have not been included in this figure.
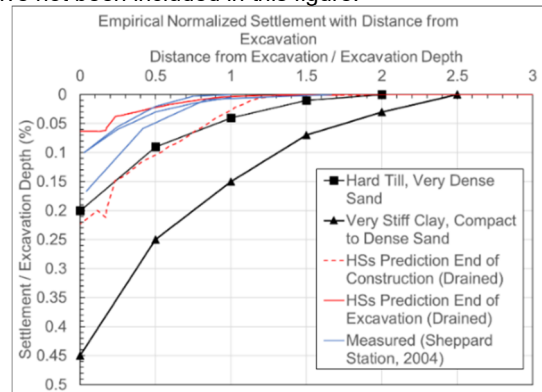

Figure 14. HSs ground surface normalized settlement plotted with empirical and historical settlement data

4.3.2   Validation against Measured Inclinometer Data

The HSs model predictions of shoring wall movements at the end of excavation (EOE) and at the end of construction (EOC) were compared with the movements measured by inclinometer for SYS (Boone and Westland, 2004) as shown in Figure 15. The maximum inclinometer deflections published by Boone and Westland (2004) were 14mm (EOE) and 30mm (EOC). The total measured lateral deformation integrated over the inclinometer depth was 0.18 m^3/m. and 0.31m^3/m. The HSs model predicted maximum horizontal movements at EOE and EOC to be 10mm and 27mm respectively for the transient seepage case. The total measured lateral deformation with depth above the base of excavation was 0.15 m^3/m at EOE and 0.35m^3/m at EOC. For the fully drained condition, the

maximum predicted horizontal movements at EOE and EOC were 13mm and 31mm respectively. The total measured lateral deformation with depth above the base of excavation was 0.18 m³/m and 0.48 m³/m. Percent errors to the SYS measured values are summarized in Table 4.

Table 4. Calculated Percent Error between HSs Prediction and Measured Result

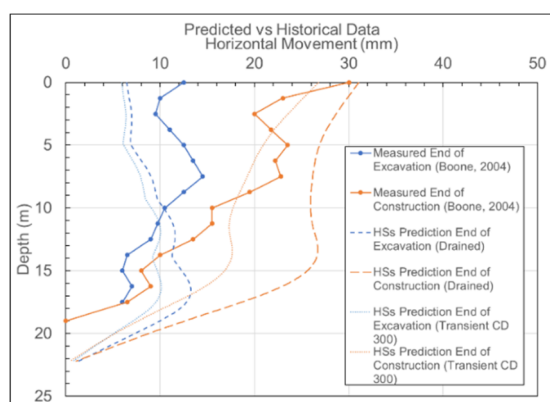| % Error	Fully Drained	Transient (CD=300)
EOE Max Deflection	-9%	-30%
EOE Lateral Volume	0%	-16%
EOC Max Deflection	4%	-11%
EOC Lateral Volume	57%	14%

Figure 15. HSs Predicted Horizontal Wall Movements plotted against measured inclinometer data for Sheppard-Yonge Station (Line 4).

5 DISCUSSION

5.1 Shear Strength
5.1.1 Undrained Shear Strength

The calibrated HSs model was shown to reasonably predict the lower bound undrained shear strength envelope from in-situ pressuremeter testing. The model generally under-predicts the in-situ pressuremeter measurements as the till deposit at FWS is heterogeneous. The PLAXIS model assumes a homogenous till and did not capture the stiffer sand and silt layers, which will exhibit greater strength.

The predicted undrained shear strength profile is compared with published data. SHANSEP analysis of clay strength is estimated by the following relationships by Ladd (1991):

$$\frac{s_u}{\sigma'_v} = S\,(OCR)^m \qquad [10]$$

where S is the ratio of shear strength over in-situ vertical effective stress at normal consolidation, and m is the power relationship with over-consolidation, which can be approximated by the following:

$$m = 0.88(1 - \frac{Cs}{Cc}) \qquad [11]$$

Using Equation 10 and 11, the predictions of the HSs model imply that a normally consolidated strength ratio, S, of approximately 0.5 for DSS, and 0.7 for CIUC. This ratio is greater than 0.45 reported for CIUC for Dublin Boulder Clay by Lehane and Simpson (2000). Note that for soft

clay, 0.25±0.05 for DSS and 0.33±0.05 were reported by Ladd (1991). The authors recommend that these ratios are to be used with caution, as the S ratios found in this study were higher than other clay soils.

5.1.2 Earth Pressure Comparison Against Empirical Apparent Earth Pressure

The HSs model predictions for earth pressure for SYS matches the local empirical apparent earth pressure diagrams in the top 12m. Below 12m, the model predicts higher earth pressure, as shown in Figure 16.

The Halton tills in Toronto exhibit stress dependency of stiffness with effective stress. As the HSs model accounts for this stress dependency, the soil at greater overburden depths were simulated with greater stiffness and strength. In the SYS model, the bottom of the excavation has not yielded, which results in less total stress redistribution to the pile wall toe. By contrast, the empirical apparent earth pressure diagrams assume the earth loads are redistributed between the struts and the pile toe. It should be noted that the apparent earth pressure diagrams do not account for the relative stiffness between the wall, and soil. As such, the diagrams are not capable of predicting whether the total stresses around the excavation can be redistributed. Therefore, in cases where the excavations are deep in Halton Till, the apparent earth pressure diagram would under-predict the earth pressures, and lead to non-conservative retaining wall designs.
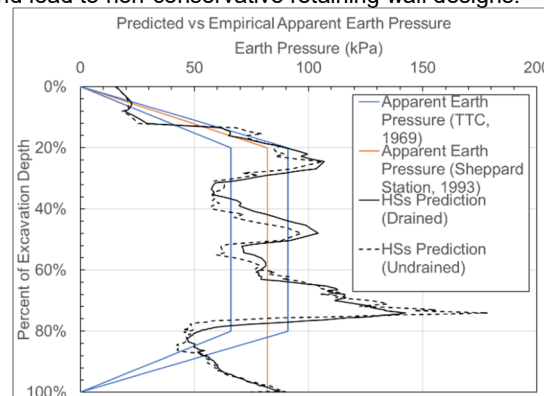

Figure 16. HSs predicted earth pressures plotted against empirical TTC apparent earth pressure diagrams

5.2 Ground Movements and Stiffness

The calibrated HSs model was capable of predicting preliminary estimates of ground movements for a similar project (i.e. SYS) in Halton tills in Toronto. The surficial ground settlement predictions were compared against the local normalized settlement curves. A maximum settlement of 0.2% is compatible with local experience.

The HSs model was generally capable of predicting the maximum magnitude of wall movements of measured inclinometer data from SYS. However, there were higher errors on the deflected shape and total lateral deformations when compared to measurements from SYS.

A factor contributing to the discrepancy is the differences in geological deposits between FWS and SYS. It should be noted that Boone and Westland (2004) present

friction angles of 38° for the glacial till, 36°, for the sand and silt layers. These values are higher than the values measured at FWS for the glacial till. The SYS higher reported values and FWS lower calibrated friction angles would lead to over predictions of deformations with depth, which was observed in the results. Despite these differences, the predictions of the model calibrated to soil data from Finch West Station, can reasonably match the maximum horizontal and vertical movements of the ground.

Another factor contributing to the differences is the assumptions made regarding the construction sequence at SYS. The model predicted drained movements at the EOE is a better match to the site measurements from inclinometer than the transient analysis predictions. This suggests that the excavation phases progressed slowly enough for excess porewater pressures to dissipate and it represents nearly drained conditions. This observation is supported by the evidence in the historical paper which show that the duration to install the three levels of struts was approximately 180 construction days. Conversely, the construction phases between EOE and EOC progressed relatively faster, and therefore the transient analysis was a closer to the site measurements than the drained predictions.

6 CONCLUSION

This paper shows that the advanced HSs model can be calibrated from conventional laboratory and test data, when interpreted in conjunction with knowledge of the local geology. The paper shows the derivation of each parameter for the HSs model.

The calibrated HSs model reasonably predicts the lower bound shear strength envelope compared with in-situ pressuremeter test. The model's earth pressure predictions compared with empirical apparent earth pressure diagrams are relatively similar in the top 12m. However, the apparent earth pressure diagram may under-predict earth pressures at depths greater than 12m.

The stiffness and ground movement predictions from the model are generally in good agreement with local empirical experience and measured data from a similar historical project in Toronto Halton Till. Despite several modelling assumptions and differences in geological stratigraphy, it was demonstrated that the carefully calibrated HSs model from FWS can reasonably predict ground movements for a project in Toronto.

Future work on this topic is to compare the predictions of the calibrated HSs model to site-specific instrumentation and monitoring data from FWS. Additional small strain soil testing, and cyclic triaxial testing is recommended to obtain site-specific shear strain degradation for small strain dynamic analysis, and E_{ur} parameters directly for future projects.

7 ACKNOWLEDGMENT

8 REFERENCES

Bolton, M.D. 1986. The Strength and Dilatancy of Sands: *Geotechnique 36.* No.1, 65-78

Boone, S.J., and Westland, J. 2004. Design Construction and Performance of a Deep Braced Excavation. Proceedings: *Fifth Internation Conference on Case Histories in Geotechnical Engineering.*

Boone, S.J., Garrod, B., and Branco, P. 1998. Building and Utility Damage Assessments, Risk and Construction Settlement Control. *Tunnels and Metroplolises,* Balkema, Rotterdam, 243 -248.

Cao, L. 2015. Engineering characteristic of glacial tills in GTA Proceedings: *GeoQuebec. Canadian Geotechnical Society Conference*

Clough, W.G., and O'Rourke, T.D. 1990. Construction Induced Movements of Insitu Walls, Design and Performance of Retaining Structures, ASCE. 439-469

Ladd, C.C. 1991. Stability evaluation during staged construction (22nd Terzaghi Lecture). *J. of Geotech. Eng.*, 117(4), 540-615.

Lehane, B., and Simpson, B. 2000. Modelling glacial till under triaxial conditions using a BRICK soil model. *J. Geotech. Eng*. Div., 106(11), 1219-1242.

Naghavi, N., Moghaddam, R., Walters, D., and Creer, G. 2019. A comparison between free-field shear strain profiles using natural and synthetic earthquake motions in a case study. Proceedings: *GeoSt.Johns Canadian Geotechnical Society Conference*

Obrzud, R.F., and Truty, A. 2018: The Hardening Soil Handbook – A Practical Guidebook, Zace Services

Schanz T., Vermeer, P.A., Bonnier, P.G. 1999. *Beyond 2000 in Computational Geotechnics – 10 Years of PLAXIS.*

Santos J.A., and Correia A.G. 2001. Reference threshold shear strain of soil, it's application to obtain a unique strain-dependent shear modulus curve for soil. Proceedings: 15th International Conference on Soil Mechanics and Geotechnical Engineering.

Vardanega. P.J., Bolton, M.D. 2011. Practical methods to estimate the non-linear stiffness shear stiffness of fine-grained soils. International Symposium on Deformation Characteristics of Geomaterials

TTC. 1967. Lateral Earth Pressure Studies on Strutted Excavations of the Toronto Subway System. Toronto Transit Commission.